ELSEVIER

Journal of Power Sources 52 (1994) 185–192

JOURNAL OF POWER SOURCES

Determination of thermodynamic, kinetic and interfacial properties for the Li//$Li_xMn_2O_4$ system by electrochemical techniques ☆

J. Barker, R. Pynenburg, R. Koksbang

Valence Technology Inc., 6781 Via Del Oro, San Jose, CA 95119, USA

Received 17 January 1994; accepted in revised form 14 June 1994

Abstract

Thermodynamic, kinetic and impedance studies of the Li//$Li_xMn_2O_4$ (spinel phase) have been carried out using a polymer-based electrolyte system. There appear to be three voltage ranges for the reversible lithium intercalation reaction, centered around 4, 2.9 and 1.1 V versus Li/Li^+. A cell utilizing all three ranges shows good coulombic reversibility but also relatively high cell impedance at the lower cell voltage. The upper voltage range shows excellent reaction kinetics, good coulombic reversibility and low cell impedance. A third and previously unidentified structural or electronic modification in the spinel phase has been found at about 3.9 V versus Li/Li^+. The 2.9 V plateau is characterized by reasonable coulombic reversibility, slower reaction kinetics and higher cell impedance than the upper voltage region. The voltage region around 1.1 V versus Li/Li^+ is considered too low for practical application.

Keywords: Lithium; Manganese; Interfacial properties

1. Introduction

High voltage cathode materials for use in lithium-based secondary battery systems have been of considerable interest in recent years [1–3]. In particular, these materials may find application in the so-called 'rocking-chair' or 'lithium ion' batteries incorporating carbon-based anodes [4]. To date, the candidate cathode materials include Li_xCoO_2 [5–7], $Li_xMn_2O_4$ [8,9], Li_xNiO_2 [10,11] and $Li_xNi_{0.5}Co_{0.5}O_2$ [12,13]. The Li_xCoO_2 material has already found application in one successful commercial product [14–16]. However, for many practical applications this material is considered relatively expensive and considerable effort has also been made in optimizing the more cost-effective $Li_xMn_2O_4$ material [17]. This material has a spinel framework structure consisting of a cubic-closed packed oxide ion lattice [18,19]. It is reported that the framework structure has accessible sites for reversible electrochemical intercalation such that the material can insert and liberate lithium over the composition range $0<x<2$ [8]. This is the basis for its use in secondary battery systems.

Li//$Li_xMn_2O_4$ electrochemical cells using lithium metal anodes in a suitable plasticized polymer electrolyte system should allow the electrochemical characterization of the spinel phase $Li_xMn_2O_4$. The polymer electrolyte system used in this work has several key advantages over conventional liquid-based electrolytes, some of which have been described in detail elsewhere [20,21]. In this paper detailed electrochemical measurements have been used to generate thermodynamic, structural, kinetic and interfacial information for the system.

2. Electrochemical voltage spectroscopy

Thermodynamic, kinetic and order/disorder information were recorded using the electrochemical voltage spectroscopy, EVS technique. EVS was originally devised by Thompson [22,23] to investigate lithium intercalation reactions in the layered chalcogenide TiS_2. It has also been used fairly extensively to study ion-insertion reactions in conducting polymer systems [24]. EVS is a voltage-step technique which provides a high resolution approximation to the open-circuit voltage (OCV) discharge curves for the complete electrochemical cell under investigation. The technique initially involves the measurement of the cell current resulting

☆ Part of the EVS data were presented at the IBA Fall Meeting, New Orleans, LA, USA, Oct. 1994.

SSDI 0378-7753(94)01958-X

from the application of a small potential step, dV, to the cell. The current is continuously monitored until it decays to a pre-set minimum value, I_{lim}. The cell potential is then stepped by dV again. The value of I_{lim} is chosen such that the cell is close to thermodynamic equilibrium at the end of the current transient to ensure that voltage corrections due to the cell IR drop and diffusion overvoltages are insignificant. During each step the current is integrated to allow calculation of the differential capacity, dx/dV, where x is the lithium ion concentration in, for example, $Li_xMn_2O_4$. The differential capacity data have demonstrated to allow effective characterization of order/disorder and structural ordering phenomenon in intercalation systems [25,26].

EVS has recently been extended to yield kinetic data for the intercalation reactions [27]. The decay of the cell current following a voltage step is proportional to $t^{-1/2}$ for linear diffusion in a semi-infinite system [28]. The apparent chemical diffusion coefficient, D, for the composite electrode, can then be calculated at each voltage increment by application of the standard Cottrell equation [29]. The validity of these measured diffusion coefficients was confirmed by measurements on similar cells by application of a current-step/potential transient method, the so-called galvanostatic intermittent titration technique (GITT), described in detail in Ref. [30].

3. Experimental

The electrochemical measurements were carried out under thermostatic conditions at 23 °C. All the cell cycling experiments requiring instrument control were performed using custom software written in HP Instrument Basic in conjunction with the standard HP-IB (IEEE-488) parallel interface bus. The EVS experiments were performed using either an Advantest R6142 precision voltage source/sink coupled to a HP Model HP3144A digital multimeter, or alternatively a Schlumberger Instruments Model 1286 electrochemical interface. The GITT experiments were conducted using the Model 1286 coupled to the Model HP3144A for voltage transient measurements. The constant-current cycling and current-interrupt experiments were carried out using the Model 1286. The constant-current cycling conditions were 0.25 mA cm^{-2} for both cell charge and discharge.

The a.c. impedance measurements were performed using the Schlumberger Instruments Models 1286 electrochemical interface and 1255 frequency response analyzer. Data analysis was carried out using the conventional Schreiber Associates Zplot software. The frequency limits were typically set between 65 kHz to 0.1 Hz, and the a.c. oscillation was ± 10 mV.

The $Li_xMn_2O_4$ was prepared by heating appropriate amounts of thoroughly mixed MnO_2 and Li_2CO_3 to 800 °C for 48 h in open air. The phase purity of the compound was examined by powder X-ray diffraction (XRD) using a Siemens D5000 powder diffractometer and Cu Kα radiation. As seen in Fig. 1, a highly crystalline material was obtained and all XRD lines were identified as belonging to the $LiMn_2O_4$ spinel phase. The $LiMn_2O_4$ spinel crystallizes in the cubic $Fd3m$ space group ($Z=8$). The refined unit cell is 8.227(2) Å and the unit cell volume is 556.83 $Å^3$, which compare well with literature data in Ref. [31].

A polymeric electrolyte, prepared by radiation polymerization as described elsewhere [20,21], was used as both the electrode separator and the binder in the composite electrodes. The room temperature conductivity of the electrode exceeds 1 mS cm^{-1} and the salt diffusion coefficient was found to be in the range from 10^{-6} to 10^{-5} cm^2 s^{-1}. Thus, the electrical properties of the electrolyte are comparable with those of commonly used liquid electrolytes [32]. The influence of the transport properties of the electrolyte on the transport properties of the test cells is considered to be insignificant.

The cell construction has been described previously [20,21] and consists of a $Li_xMn_2O_4$-containing cathode, and a metallic lithium anode, separated by the polymeric electrolyte, placed in a flexible encapsulation which is heat-sealed under vacuum.

Particle size determination was carried out with a Coulter Multisizer II, which was set up to measure in the 2–60 μm range and the results were confirmed with a Microtec UPA particle size analyzer which is used for measuring particle sized below 6 μm. The measurements indicated an average particle size of around 4 μm for the $Li_xMn_2O_4$.

The atomic absorption measurements were conducted using an Instrumentation Laboratory AA/AE spectrophotometer Model 357 with a manganese specific Westinghouse Model WL22936 hollow cathode lamp used at 5 mA and 279.5 nm.

4. Results and discussion

The as-prepared spinel phase was chemically analyzed by atomic absorption (AA) to give the approximate composition $Li_{1.05}Mn_2O_4$. $Li//Li_xMn_2O_4$ cells made from this material showed an initial, stable OCV of around 3.1 V versus Li/Li^+. For cycling investigations using cells in the fully charged state, these cells were electrochemically oxidized to a stable OCV of approximately 4.3 V versus Li/Li^+ using the EVS technique. This ensured that the cells were close to thermodynamic equilibrium during the charge procedure which minimized the risk of electrochemical oxidation of the

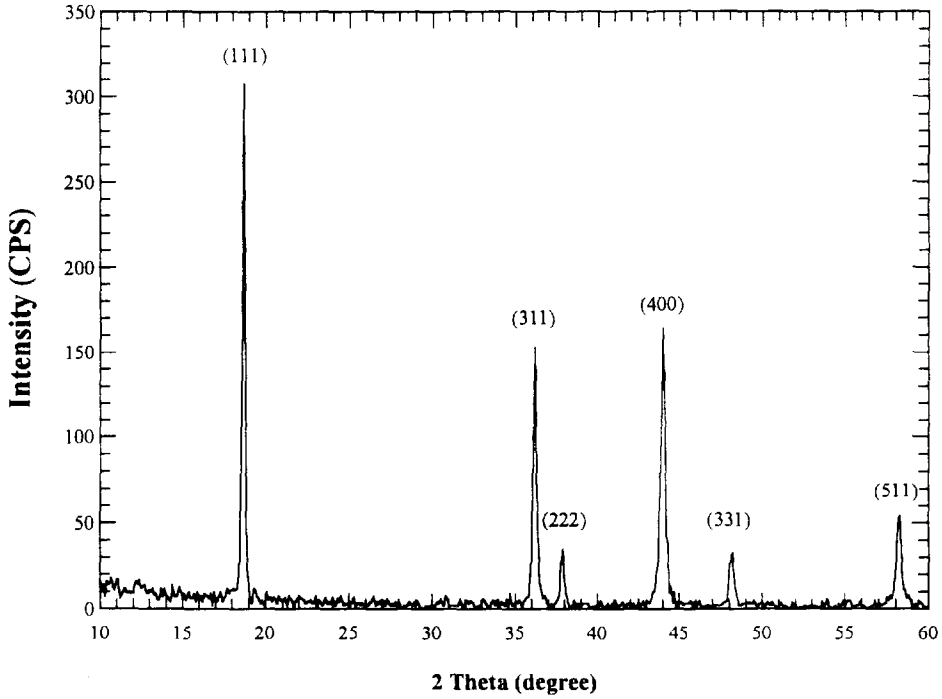

Fig. 1. Indexed powder X-ray diffraction diagram of $LiMn_2O_4$.

electrolyte. This process electrochemically extracted lithium from the parent spinel. The charge passed during this stage suggested that the fully charged state corresponded to the approximate cathode composition $Li_{0.20}Mn_2O_4$ (i.e., the recently reported λ-MnO_2 phase [33]).

Fig. 2 shows the constant-current cycling (cycles 1 and 5) voltage profiles, starting from a fully charged $Li//Li_xMn_2O_4$ cell, shown as a function of the lithium intercalation concentration, x. Three distinct regions are observed corresponding to the reported structural phase changes occurring in the $Li_xMn_2O_4$ during cell discharge [34] i.e., cubic to tetragonal to trigonal [35]. It is noteworthy that the insertion reaction appears to be coulombically reversible over the entire concentration range $0<x<4$, although some small changes are seen. For instance, the voltage curves seem to smoothen upon cycling and a minor fraction of the reversible capacity is lost. A significant hysteresis due to pronounced cell overvoltage is also observed, notably on the two lower voltage plateaus. The increased overvoltage and the smoothening of the voltage curves, observed during cycle 5, are presumably associated with some minor modification in the structural integrity of the $Li_xMn_2O_4$ which occurs during the lithium intercalation/de-intercalation reactions.

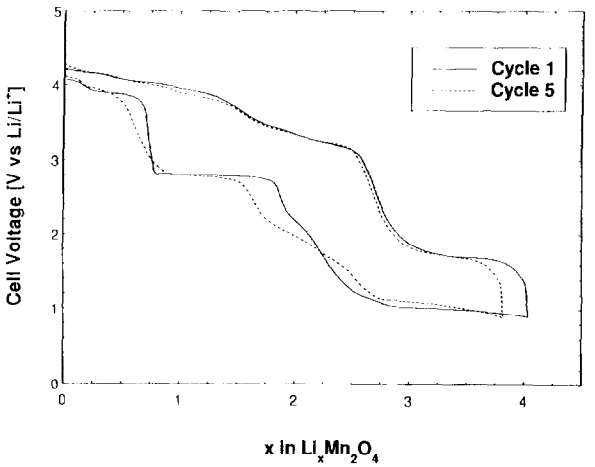

Fig. 2. Voltage profiles of the cycles 1 and 5 from cell constant current cycling (0.25 mA cm^{-2} charge and discharge) for the $Li//Li_xMn_2O_4$ system in the voltage range from 1.0 to 4.3 V.

The remaining part of this paper concentrates on the two upper voltage regions shown in Fig. 2. Thus it is only concerned with the cubic to tetragonal phase changes, i.e., within the insertion range $0<x<1.8$, under the prevailing test conditions. This reaction is shown to be highly coulombically reversible, and the hysteresis on the upper voltage region is very low.

Results from EVS cycle 1 measurements, for the 4.3–3.0 V voltage range are depicted in Fig. 3. For all EVS figures the reduction (i.e., lithium intercalation) reaction is shown below the x-axis. The voltage profile indicates the excellent coulombic reversibility for the system and the small amount of hysteresis between the discharge/charge curves is indicative of the low overvoltage for the associated intercalation/de-intercalation reactions within this voltage range. The differential capacity plot shows, very clearly, the two-phase behavior of this voltage range as two reversible peaks are observed.

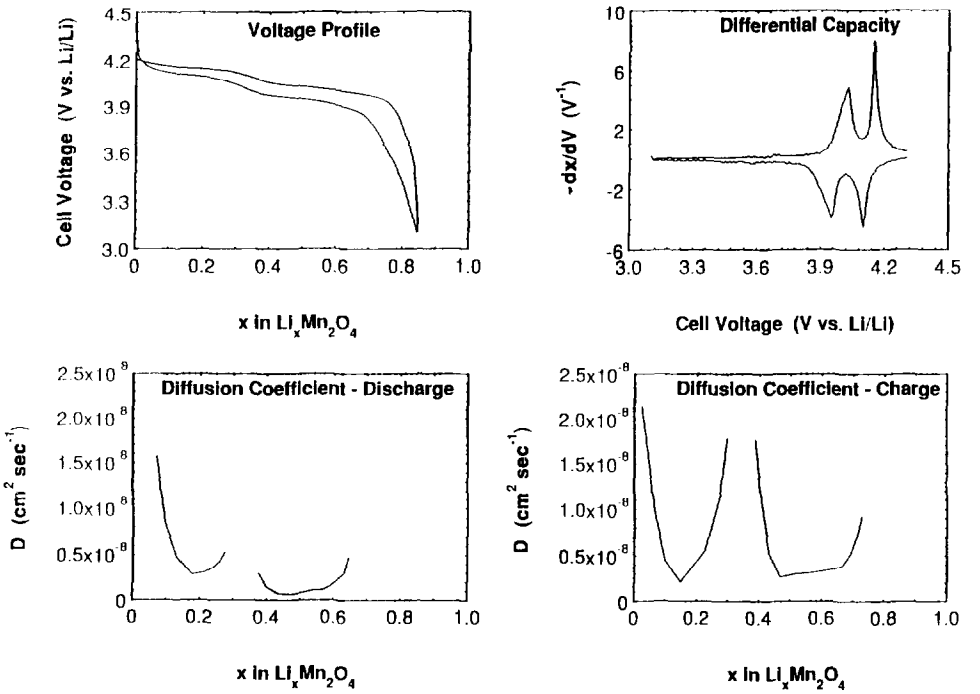

Fig. 3. Voltage profile, differential capacity and diffusion coefficient data from the EVS cycle 1 for the Li//$Li_xMn_2O_4$ system in the voltage range from 3.1 to 4.3 V.

On each plateau, a minimum in the diffusion coefficient is observed, just below $x=0.2$ and around $x=0.5$ for both charge and discharge. The presence of the kinetic minima corresponds, we suspect, to the Li–Li ionic coulombic repulsion effects within each structural site in the host lattice. Diffusion coefficients of the order of about 10^{-8} cm^2 s^{-1} are observed, which is about an order of magnitude higher than previously disclosed by Guyomard and Tarascon [36] for the $Li_xMn_2O_4$ system. The difference may be explained in terms of the varying electrode fabrication methods used in each study. The effects can distinctly affect the kinetic measurements on the active material. Furthermore, it should be noted that the diffusion coefficient calculations in this work are based on geometric electrode surface area whereas Guyomard and Tarascon [36] used an estimation of the total surface area of the cathode material. However, the variations of the intercalation kinetics with lithium ion concentration found during this study are still valid. Complementary measurements carried out on equivalent cells using the GITT method (not shown) confirm both the magnitudes of the diffusion coefficients as well as the variation with lithium ion concentration.

Similar plots for EVS cycle 2, are shown in Fig. 4, and for cycle 5 in Fig. 5. The magnitude of the diffusion coefficient seems to be unaffected by the cycling of the cell, although the minima are displaced towards lower x values, consistent with the small loss in discharge capacity over this cycle range. However, the most interesting feature of the differential capacity plots, is the presence of an additional peak at around 3.9 V versus Li/Li$^+$ (discharge) which indicates the appearance of a new structural or electronic modification. The lithium insertion reaction in this modification is reversible, although it is observed only as a shoulder on the charge curve. It is however clearly distinguishable during the EVS cycle 5 data. To our knowledge, no information regarding this new modification appears in the open literature.

EVS data are given in Figs. 6 to 8 for the cubic/tetragonal phase transformation, i.e., covering the cell voltage range 3.2 to 2.0 V versus Li/Li$^+$. Data for cycles 1, 2 and 5 are presented. The cycle 1 EVS voltage profile indicates a distinct cathodic displacement and a sharp peak at around 2.85 V versus Li/Li$^+$. We believe this peak is consistent with an overvoltage associated with the cubic to tetragonal phase change. As can be seen by inspection of the cycle 2 EVS data, a small residual overvoltage is still present even after the cell has been cycled. During cycle 5, however, the overvoltage has been totally removed, and the system shows improved reversibility.

The hysteresis of the voltage profiles indicates that this reaction is less reversible than the intercalation reactions associated with the higher voltage range. This is more clearly shown by the increased separation of the cathodic and anodic peaks in the differential capacity plots. The variation of the diffusion coefficients with degree of insertion shows a single, wide minima in this voltage range consistent with the filling/removal of one site within the host lattice. The magnitude of the

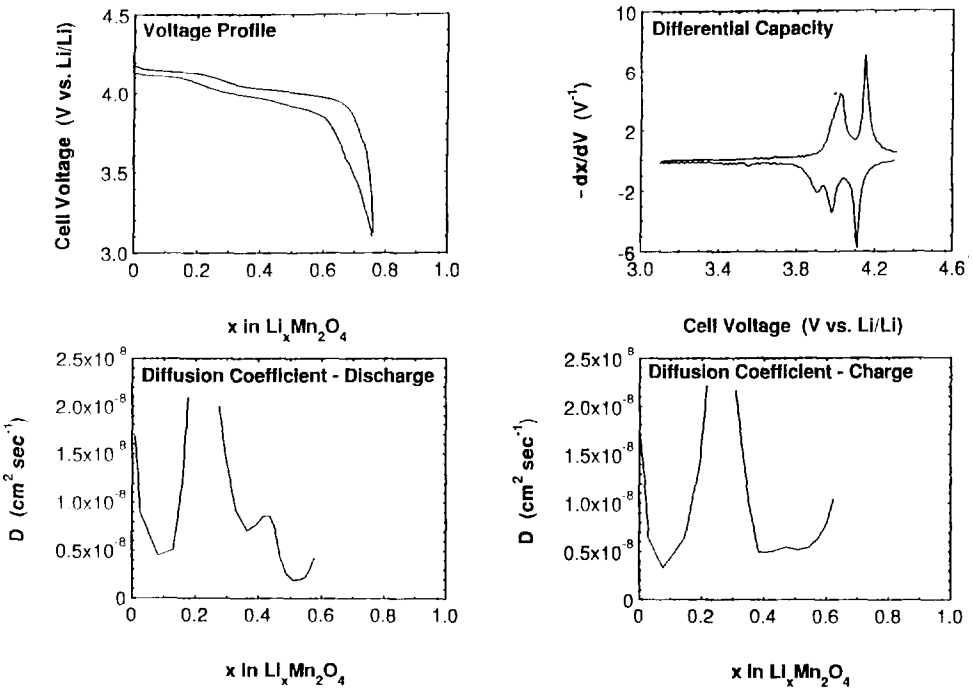

Fig. 4. Voltage profile, differential capacity and diffusion coefficient data from the EVS cycle 2 for the Li//$Li_xMn_2O_4$ system in the voltage range from 3.1 to 4.3 V.

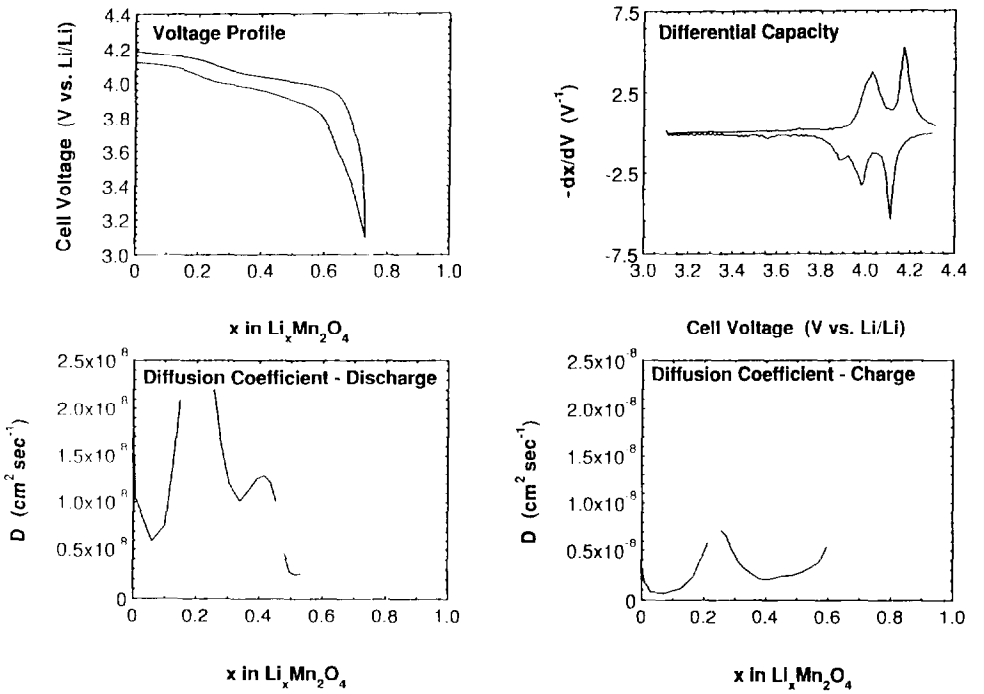

Fig. 5. Voltage profile, differential capacity and diffusion coefficient data from the EVS cycle 5 for the Li//$Li_xMn_2O_4$ system in the voltage range from 3.1 to 4.3 V.

diffusion coefficients are generally around one order of magnitude lower than those measured on the higher voltage range, i.e., around 10^{-9} cm^2 s^{-1}. Again, we believe the presence of the minima in the kinetic data is consistent with the coulombic repulsion effects expected during the filling/removal of the sites within the $Li_xMn_2O_4$. As previously mentioned, the validity of the diffusion coefficient measurements were confirmed by separate measurements using the GITT method. During cycling, the cell overvoltage decreases slightly but unfortunately this is accompanied by a decrease in the measured discharge capacity.

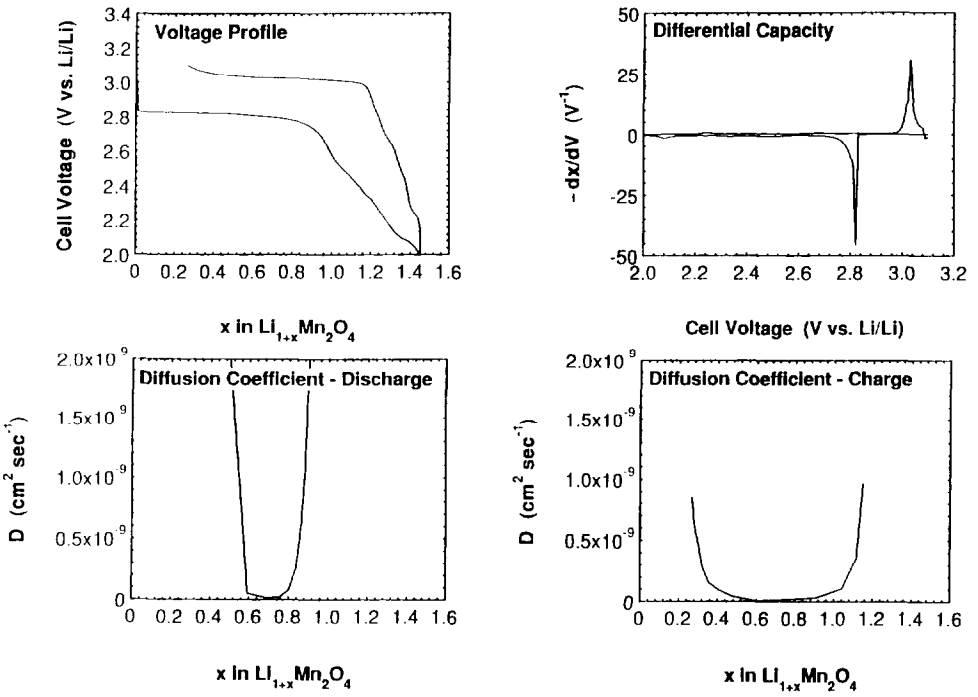

Fig. 6. Voltage profile, differential capacity and diffusion coefficient data from the EVS cycle 1 for the Li//$Li_{1+x}Mn_2O_4$ system in the voltage range from 2.0 to 3.1 V.

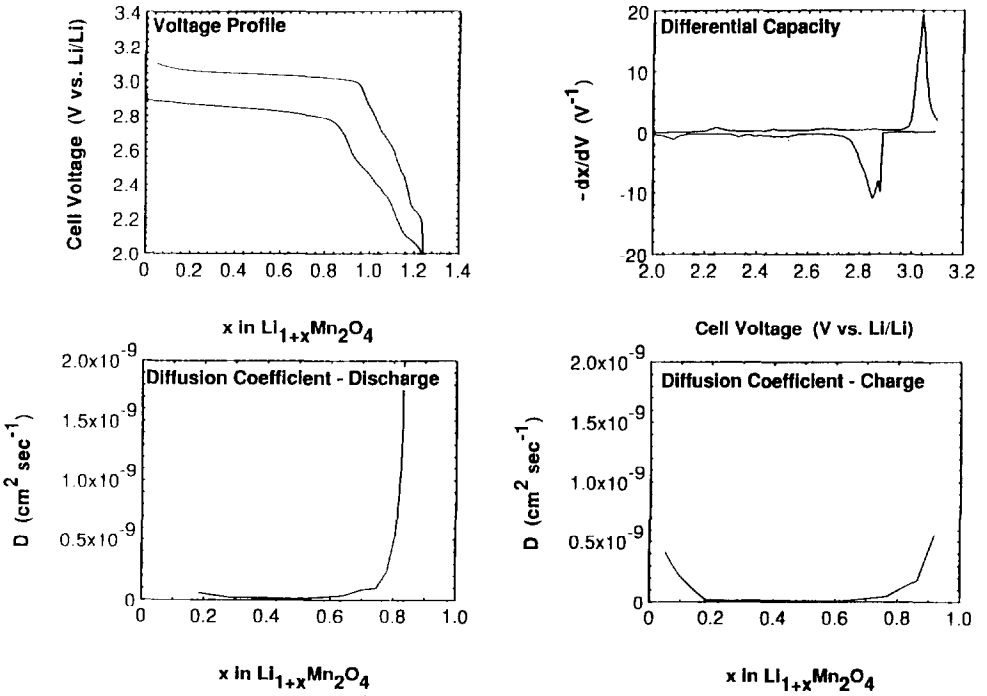

Fig. 7. Voltage profile, differential capacity and diffusion coefficient data from the EVS cycle 2 for the Li//$Li_{1+x}Mn_2O_4$ system in the voltage range from 2.0 to 3.1 V.

The d.c. cell impedance, measured by the current-interrupt technique described in Section 3, for the voltage range 4.3 to 2.0 V is shown in Fig. 9. These measurements indicate two distinct regions; the cell impedance being much lower in the high voltage range than at the lower voltage region. There is an abrupt, but reversible transition in cell impedance between the two regions. We believe the magnitude of the cell impedance is dominated by the lithium–electrolyte interfacial impedance. This has been confirmed by preliminary studies of three electrode cells which allows de-convolution of the individual electrode impedances.

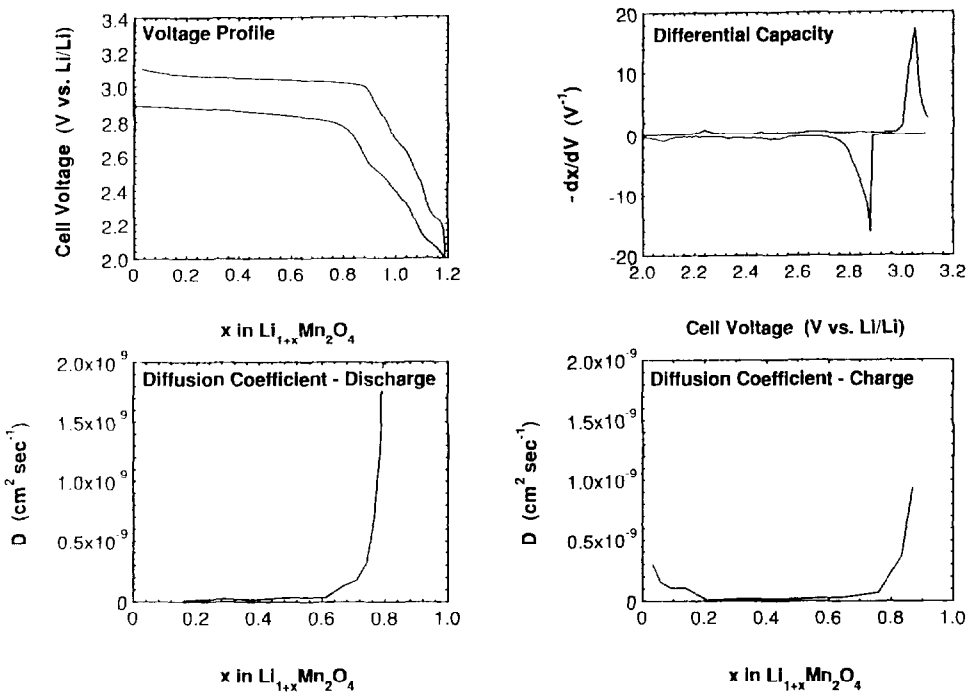

Fig. 8. Voltage profile, differential capacity and diffusion coefficient data from the EVS cycle 5 for the $Li//Li_{1+x}Mn_2O_4$ system in the voltage range from 2.0 to 3.1 V.

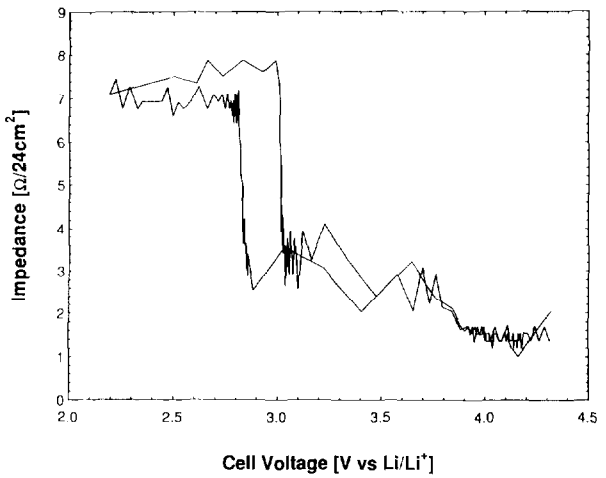

Fig. 9. Cell impedance measurement using the current-interrupt method for the $Li//Li_xMn_2O_4$ system in the voltage range from 2.2 to 4.3 V.

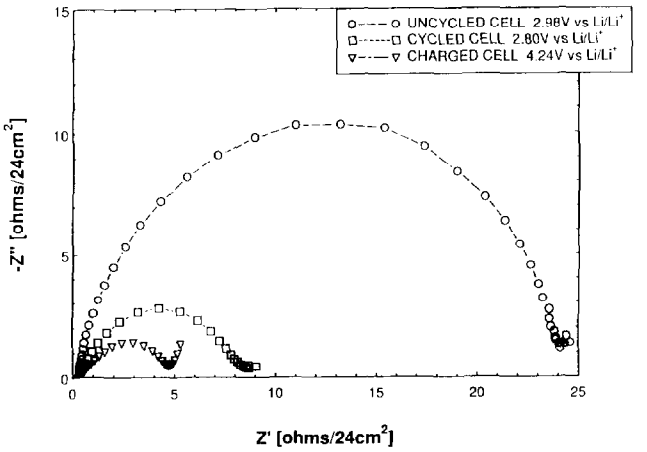

Fig. 10. A.c. impedance measurements for an uncycled cell, cycled cell, and charged cell for the $Li//Li_xMn_2O_4$ system.

The high impedance on the lower voltage region can explain, at least partly, the observation of increased hysteresis on this voltage region during constant current cycling experiments.

A.c. impedance measurements (Fig. 10), show an initially high impedance caused by the pristine oxide layer present on the as-received lithium foil. Once current is passed through the cell, this layer is removed and a lower impedance is observed, reflecting the creation of a new interfacial layer on the lithium electrode. After the first measurement, the impedance is clearly dependent on the state-of-charge of the cell, and confirm the current-interrupt measurements, i.e., high cell impedance at the low voltage plateau and low cell impedance at the high voltage plateau.

5. Conclusions

The $Li//Li_xMn_2O_4$ system has been characterized by electrochemical measurements that have generated detailed thermodynamic, kinetic and impedance results. There are three reversible voltage regions for the sequential filling and removal of sites within the host material. These are centered around 4, 2.9 and 1.1 V versus Li/Li^+. These regions correspond to literature

reported phase changes in the $Li_xMn_2O_4$ host. A cell utilizing all three voltage regions showed good reversibility but coupled to poor cell overvoltage. This later point, together with the low voltage of the last plateau, would limit its potential use.

The upper voltage region is characterized by good reaction kinetics, excellent coulombic reversibility, and a low cell impedance. These properties, coupled with a reasonable recharge capacity in this region, make this a viable material for a high cell voltage application. In particular, the material seems well suitable for incorporation in rocking-chair technology when used in conjunction with carbon-based anodes. The EVS studies indicate that there appears to be a third, previously unidentified structural or electronic modification in the spinel phase at about 3.9 V versus Li/Li^+ (discharge). The insertion reaction in this modification appears to be reversible. The precise structural phase, however, has yet to be established for this modification.

The 2.9 V voltage plateau is characterized by a two-phase region for the lithium insertion/de-insertion reaction. This corresponds to the reported cubic to tetragonal phase change in the $Li_xMn_2O_4$ material. This feature generates a single reversible peak in the differential capacity plot and a plateau in the voltage profile. The insertion reaction shows reasonable coulombic reversibility which improves with cycle number. An overvoltage is required for the structural phase change which causes a small, but distinguishable cathodic displacement in the voltage curve and a sharp peak in the differential capacity plot at around 2.85 V versus Li/Li^+. Overall, this voltage plateau shows slower reaction kinetics than the higher voltage range (shown by the comparative diffusion coefficient measurements) and also higher cell impedance. It is likely, however, that the main cause of higher cell impedance may be associated with changes at the lithium electrode rather than in $Li_xMn_2O_4$.

The cell voltage plateau around 1.1 V versus Li/Li^+, associated with the tetragonal to trigonal phase change in the $Li_xMn_2O_4$, is probably too low for practical application. Cell cycling, which includes this voltage region, appears to cause significant structural modification in the cathode as evidenced by the increased hysteresis and smoothening of the voltage inflections in the voltage–composition profile.

References

[1] J.M. Tarascon, *J. Electrochem. Soc., 132* (1985) 2089.

[3] M. Armand, in D.W. Murphy, J. Broadhead, B.C. H. Steele (eds.), *Materials for Advanced Batteries,* Plenum, New York, 1980.

[3] J.J. Auborn and Y.L. Barbario, *J. Electrochem. Soc., 134* (1987) 638.

[4] T. Nagaura, *Prog. Batteries Battery Mater., 10* (1991) 209.

[5] K. Mizushima, P.C. Jones, P.C. Wiseman and J.B. Goodenough, *Mater. Res. Bull., 15* (1980) 783.

[6] C. Delmas, C. Fouassier and P. Hagenmuller, *Mater. Sci. Eng., 31* (1977) 297.

[7] J. N. Reimers and J.R. Dahn, *J. Electrochem. Soc., 139* (1992) 2091.

[8] J.M. Tarascon, E. Wang, F.K. Shakoohi, W.R. McKinnon and S. Colson, *J. Electrochem. Soc., 138* (1991) 2859.

[9] J.N. Reimers, J.R. Dahn and U. von Sacken, *J. Electrochem. Soc., 140* (1993) 2752.

[10] M.M. Thackeray, P.J. Johnson, L.A. de Picciotto, P.G. Bruce and J.B. Goodenough, *Mater. Res. Bull., 19* (1984) 179.

[11] J.R. Dahn, U. von Sacken and C.A. Michal, *Solid State Ionics, 44* (1990) 87.

[12] T. Ohzuku, A. Ueda and M. Nagayama, *J. Electrochem. Soc., 140* (1993) 1862.

[13] C. Delmas and I. Saadoune, *Solid State Ionics, 53–56* (1992) 370.

[14] T. Ohzuku, H. Komori, M. Nagayama, K. Sawai and T. Hirai, *J. Ceram. Soc. Jpn., 100* (1992) 349.

[15] S. Mashiko, M. Yokogawa and T. Nagaura, in *Abstr. 32nd Battery Symposium, Kyoto, Japan, Apr. 1991.*

[16] K. Tanaka, M. Itabashi, M. Aoki, S. Hiraka, M. Kataoka, S. Fujita, K. Sekai and K. Ozawa, *Ext. Abstr., Electrochemical Society Meet., New Orleans, LA, USA,* Oct. 1993.

[17] T. Nagaura and T. Rozawa, *Prog. Batteries Solar Cells, 9* (1990) 209.

[18] J.M. Tarascon and D. Guyomard, *J. Electrochem. Soc., 138* (1991) 2864.

[19] A.F. Wells, *Structural Inorganic Chemistry,* Oxford University Press, London, 4th edn., 1975, pp. 466–431.

[20] J.S. Lundsgaard, S. Yde-Andersen, R. Koksbang, D.F. Shackle, R.A. Austin, D. Fauteux, in B. Scrosati (ed.), *Proc. 2nd Int. Symp. Polymer Electrolytes,* Elsevier Applied Science, London, 1990, p. 395.

[21] R. Koksbang, F. Flemming, I.I. Olsen, P.E. Tonder, K. Bondum, M. Consigny, K.P. Perterson, S. Yde-Anderson, in K.M. Abraham and M. Saloman (eds.), *Proc. Symp. Primary and Secondary Lithium Batteries,* Proc. Vol. 91-3, The Electrochemical Society, Pennington, NJ, USA, 1991, p. 157.

[22] A.H. Thompson, *Phys. Rev. Lett., 23* (1978) 1511.

[23] A.H. Thompson, *J. Electrochem. Soc., 126* (1979) 608.

[24] J. Barker, *Synth. Met., 32* (1989) 43.

[25] T. Jacobson, K. West and S. Atlung, *J. Electrochem. Soc., 126* (1979) 608.

[26] O. Tillement and M. Quarton, *J. Electrochem. Soc., 140* (1993) 1870.

[27] J. Barker, D. Baldwin, D.C. Bott and S.J. Porter, *Synth. Met., 28* (1989) D127.

[28] W. Jost, in *Diffusion in Solids, Liquids and Gases,* Academic Press, London, 1952.

[29] A.J. Bard and L.R. Faulkner, *Electrochemical Methods: Fundamentals and Applications,* Wiley, New York, 1980, pp. 142–146.

[30] W. Weppner and R.A. Huggins, *J. Sol. State Chem., 22* (1977) 297.

[31] A. Mosbah, A. Verbaere and M. Tournoux, *Mater. Res. Bull., 18* (1983) 1375.

[32] H.V. Venkatasetty (ed.), *Lithium Battery Technology,* Wiley, New York, 1984, p. 39.

[33] J.C. Hunter, *J. Solid State Chem., 39* (1981) 142.

[34] K. West, Personal communication, 1993.

[35] T. Ohzuku, M. Kitagawa and T. Hirai, *J. Electrochem. Soc., 137* (1990) 769.

[36] D. Guyomard and J.M. Tarascon, *J. Electrochem. Soc., 139* (1992) 937.